Table 1. Basic electrophysiological properties of Purkinje cells

	Membrane capacitance (pF)[a,d]	Resting membrane potential (mV)[a]	Input resistance (MΩ)[a,d]	Percentage of cells showing spontaneous action potentials[b,e]	Frequency of spontaneous action potentials (Hz)[c,e]
GFP alone	39.2 ± 24.3 (n = 35)	−58.3 ± 13.6 (n = 35)	379 ± 278 (n = 35)	80% (12 of 15 cells)	0.43 ± 1.00 (n = 15)
WT mKv3.3	40.1 ± 16.1 (n = 17)	−59.9 ± 8.24 (n = 17)	367 ± 181 (n = 17)	75% (6 of 8 cells)	0.25 ± 0.59 (n = 8)
R424H mutant	22.3 ± 6.9*† (n = 28)	−59.5 ± 7.4 (n = 28)	372 ± 169 (n = 28)	64% (9 of 14 cells)	0.12 ± 0.75 (n = 14)

Here and in Table 2, statistical analysis was conducted between cells expressing the R424H mutant and those expressing green fluorescent protein (GFP) alone or between cells expressing R424H mutant and those expressing wild-type (WT) mKv3.3. Data are given as the means ± SD, and n is the number of experiments. *$P < 0.001$ between GFP alone and R424H mutant. †$P < 0.001$ between WT mKv3.3 and R424H mutant. The statistical analysis indicated by superscript letters a, b and c was conducted using Student's unpaired t test, the χ^2 test and Mann–Whitney U test, respectively. [d]Membrane capacitance and input resistance were measured in voltage-clamp conditions. [e]Spontaneous action potentials were recorded at resting membrane potential for 300 s.

compared with PCs expressing GFP alone or those expressing WT subunits (Table 1; resting membrane potential, R424H *versus* GFP, $P = 0.533$; R424H *versus* WT, $P = 0.874$; and input resistance, R424H *versus* GFP, $P = 0.882$; R424H *versus* WT, $P = 0.913$; analyses by Student's unpaired t test). Spontaneous action potentials were also observed in some PCs in all groups (Table 1 and Supplemental Fig. S4*B* and *C*). The percentages of PCs generating spontaneous firing and the frequency of the firing were comparable among the three groups (Table 1).

Outward currents were recorded in Hepes-buffered ACSF containing TTX, $CdCl_2$, picrotoxin and DNQX (see Methods). Representative current traces recorded from GFP-, WT- and R424H mutant-expressing PCs are illustrated in Fig. 4*A*. Depolarizing voltage pulses (more positive than −10 mV) evoked outward currents with a transient peak in GFP-, WT- and R424H mutant-expressing PCs (Fig. 4*A*). In WT-expressing PCs, peak amplitudes of the transient currents were larger than those in GFP-expressing PCs, indicating that lentivirally expressed mKv3.3 formed functional channels (Fig. 4*Ab*). In contrast, the peak amplitudes in R424H mutant-expressing PCs were smaller than those in GFP-expressing PCs (Fig. 4*Aa* and *Ac*). As the membrane capacitance of R424H mutant-expressing PCs was significantly smaller than that of GFP- and WT-expressing PCs (Table 1), the peak current amplitudes at voltages between +10 and +40 mV were normalized to membrane capacitances (current densities, in pico-amperes per picofarad; Fig. 4*B*). The current densities in R424H mutant-expressing PCs were ~2-fold smaller than those in GFP-expressing PCs at voltages between +10 and +40 mV (Fig. 4*B*), confirming that the expression of the R424H mutant subunits in cultured PCs suppressed outward currents in a dominant-negative manner.

Expression of R424H mutant subunits reduces sEPSCs in PCs

In standard culture conditions, PCs receive excitatory synaptic inputs from granule cells via the dendrites (Hirano *et al.* 1986; Hirano & Kasono, 1993). In order to examine how R424H mutant-induced impairment of dendritic development affects the synaptic inputs to PCs, sEPSCs were recorded from PCs in the presence of picrotoxin at a holding potential of −80 mV (Fig. 5). Examples of sEPSCs in GFP- or WT-expressing PCs appear as downward deflections in the current traces (Fig. 5*Aa* and *Ba*). These currents were abolished by application of 20 μM DNQX (traces not shown) and were thus identified as being mediated by AMPA/kainate receptors. Ensemble averages of the events in individual cells are also shown in Fig. 5*Ab* and *Bb*. Although sEPSCs in both groups were observed in all cells tested (Table 2), most R424H mutant-expressing PCs (10 of 13 cells) did not show sEPSCs during the 250 s recording period (Fig. 5*C* and Table 2; R424H and GFP, $P < 0.001$; R424H and WT, $P < 0.001$ by Fisher's exact probability test). Even in PCs showing sEPSCs, the frequency was significantly lower than in GFP- or WT-expressing PCs (Table 2). The R424H mutant-expressing PCs might receive few, if any, excitatory synaptic contacts onto their somata and dendrites.

R424H mutant-expressing PCs exhibit broadened action potentials and altered firing patterns

Expression of R424H mutant subunits in PCs suppressed outward current density, suggesting the alteration of the action potential waveform and firing properties in R424H mutant-expressing PCs. To examine these possibilities,

single action potentials (Fig. 6) and repetitive firings (Fig. 7) were evoked in current-clamp conditions. When a single action potential was evoked by short current injection (10 ms duration), R424H mutant-expressing PCs showed a broadened action potential waveform (Fig. 6*A*). The half-amplitude widths of R424H mutant-expressing PCs were 1.7-fold larger than those of GFP-expressing PCs (Fig. 6*B*; $P < 0.001$). The maximal rate of rise and maximal rate of fall in R424H mutant-expressing PCs were 0.75- and 0.65-fold of those in GFP-expressing PCs, respectively (Fig. 6*C* and *D*; maximal rate of rise, $P < 0.001$; maximal rate of fall, $P < 0.001$). These changes suggest that not only outward K^+ current but also voltage-dependent Na^+ current (I_{Na}) was affected by the expression of R424H mutant, because the maximal rate of rise of the action potential has been used as an index of the inward I_{Na} (Hodgkin & Katz, 1949).

To clarify the reduction of the maximal rate of rise by R424H mutant expression, I_{Na} was recorded from PCs in voltage-clamp conditions (Supplemental Fig. S5). Expression of R424H mutant subunits significantly reduced I_{Na} compared with the control group, without any changes in the voltage dependence of activation and inactivation. As the I_{Na} of cultured PCs is distributed through the cell body and axons (Fry *et al.* 2007), the reduction in I_{Na} would be due to the smaller cell body (Table 1, 'Membrane capacitance') and impaired neurite extension of R424H-expressing PCs. The expression of R424H mutant subunits did not affect the threshold current, threshold potential or action potential amplitude of PCs compared with expression of GFP (Fig. 6*E–G*). These results strongly suggest that expression of R424H mutant subunits inhibited the activation of the endogenous mKv3.3 channels, resulting in a reduction of the maximal rate of fall and then in the broadening of action potential duration in PCs.

We next examined the firing properties evoked by long current injection (200 ms duration). Most GFP-expressing PCs (82.9%) showed tonic firing of action potentials (tonic type) in response to depolarizing current injection (Fig. 7*A* and filled column of GFP in Fig. 7*E*), which is consistent with previous reports on the firing pattern of cultured PCs (Tabata *et al.* 2000; Harada *et al.* 2006). The other PCs (17.1%) showed a few spikes (up to three spikes) in response to current injection ranging from 0 to 200 pA

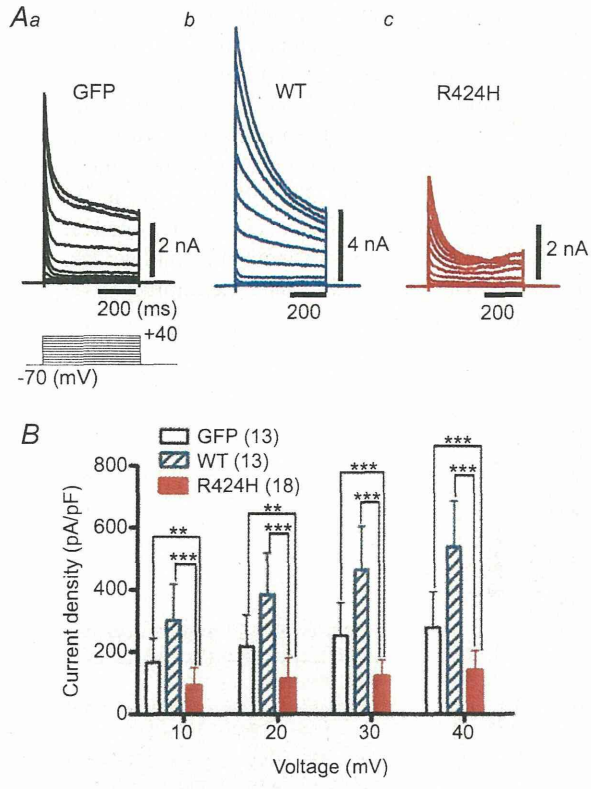

Figure 4. R424H mutant-expressing PCs exhibit suppressed peak outward current density
A, representative outward current traces recorded from PCs expressing GFP alone (*Aa*), WT subunits (*Ab*; note the vertical scale bar) and R424H mutant subunits (*Ac*). The currents were evoked by voltage steps from the −70 mV holding potential to voltages ranging from −60 to +40 mV in 10 mV increments. Leak currents were subtracted online by the *P*/4 protocol. The currents were recorded at DIV 8–10 in Hepes-buffered srtificial cerebrospinal fluid (ACSF) containing TTX, $CdCl_2$, picrotoxin and 6,7-dinitroquinoxaline-2,3-dione (DNQX). *B*, summary of the peak outward current density, which was calculated by dividing the peak outward current by membrane capacitance. $^{**}P < 0.01$ and $^{***}P < 0.001$.

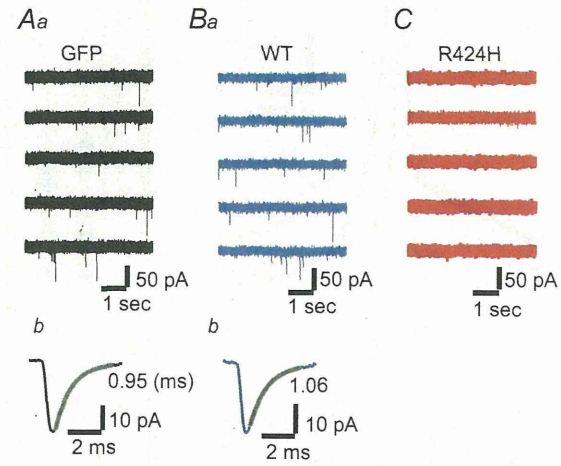

Figure 5. Absence of spontaneous excitatory postsynaptic currents (sEPSCs) in R424H mutant-expressing PCs
Aa, *Ba* and *C*, representative current traces recorded from PCs expressing GFP alone (*Aa*), WT subunits (*Ba*) or R424H mutant subunits (*C*). The sEPSCs appear as downward deflections in *Aa* and *Ba*. The PCs were held at −80 mV in the presence of picrotoxin. *Ab* and *Bb*, averaged sEPSCs from the same cell as in *Aa* and *Ba*, with superimposed single exponential fit. The decay time constant is indicated beside each trace.

Table 2. Summary of spontaneous excitatory postsynaptic current (sEPSC) properties in Purkinje cells

	Percentage of cells showing sEPSCs[a]	Amplitude (pA)[b]	Frequency (Hz)[b]	10–90% Rise time (ms)[b]	Decay time constant (ms)[c]
GFP alone	100%	33.7 ± 9.3	0.62 ± 0.35	0.18 ± 0.04	0.84 ± 0.27
(n = 15; 1502 events)	(15 of 15 cells)	(n = 15)	(n = 15)	(n = 15)	(n = 15)
WT mKv3.3	100%	34.0 ± 12.0	0.73 ± 0.35	0.19 ± 0.03	0.87 ± 0.19
(n = 10; 1041 events)	(10 of 10 cells)	(n = 10)	(n = 10)	(n = 10)	(n = 10)
R424H mutant	23%	23.1 ± 4.2	0.15 ± 0.10	0.20 ± 0.02	1.14 ± 0.21
(n = 3; 103 events)	(3 of 13 cells)**††	(n = 3)	(n = 3)*†	(n = 3)	(n = 3)

All measurements were performed at a holding potential of −80 mV. The statistical analyses indicated by superscript letters a and b were conducted using Student's unpaired t test and Fisher's exact probability test, respectively. [c]The sEPSC decay phases were fitted with a single exponential function. *P < 0.05, **P < 0.001 between GFP alone and R424H mutant. †P < 0.05, ††P < 0.001 between WT mKv3.3 and R424H mutant.

in 20 pA increments and did not fire tonically during the 200 ms depolarizing pulses (onset type; open column of GFP in Fig. 7*E*). However, approximately half of the R424H mutant-expressing PCs exhibited onset-type firing (53.6%; Fig. 7*C* and *E*), and the remaining PCs exhibited tonic-type firing (46.4%; Fig. 7*D* and *E*). The percentages of firing types in R424H mutant-expressing PCs differed significantly from those in GFP- and WT-expressing PCs (Fig. 7*E*; $P < 0.001$ in both pairs by the χ^2 test). The firing frequencies of tonic-type neurons in the three groups were plotted against the injected current (Fig. 7*F*). Wild-type-expressing PCs showed the highest frequencies, in the range of 40–200 pA (Fig. 7*B* and *F*), demonstrating that lentivirally expressed WT subunits contributed to the generation of narrow action potentials by accelerating the falling phase (Fig. 7*A* and *D* and Supplemental Fig. S3*E*). In tonic-type neurons, firing frequencies in R424H mutant-expressing PCs were significantly lower than those in GFP-expressing PCs, in the range of 180–200 pA (Fig. 7*F*; $P < 0.05$ at 180 and 200 pA depolarization). These results demonstrate that expression of R424H mutant subunits changed the ratio of tonic-firing PCs and reduced PC excitability in response to depolarization.

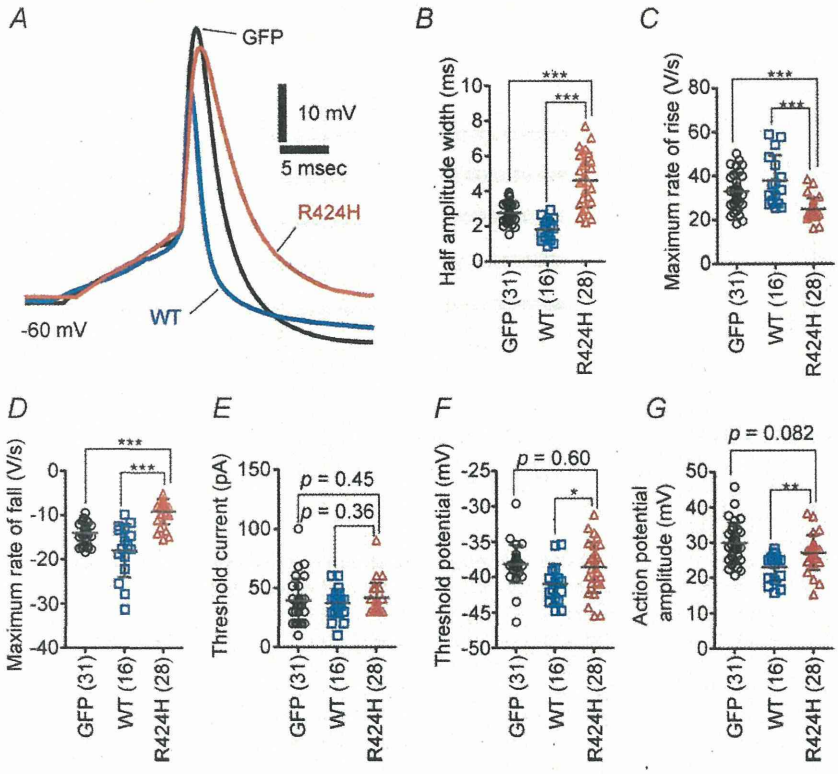

Figure 6. R424H mutant-expressing PCs exhibit broadened action potential waveforms
A, representative single action potential waveforms of PCs. The action potentials were evoked by short depolarizing current injection (10 ms duration). Action potentials were aligned by superimposing the rising phase of each trace. The resting membrane potentials were adjusted to −60 mV by current injection.
B–G, comparison of action potential properties. *B*, half-amplitude width measured at the mid-point between the threshold and peak of the action potential. *C* and *D*, maximal rate of rise (*C*) and of fall (*D*) of action potentials. *E*, threshold current amplitude. *F*, threshold potential. *G*, action potential amplitude, as measured between the threshold and peak. *P < 0.05, **P < 0.01 and ***P < 0.001.

R424H mutant-expressing PCs show higher $[Ca^{2+}]_i$, and blockade of P/Q-type Ca^{2+} channels rescues the PC death and dendritic maldevelopment caused by the mutant subunits

The expression of R424H mutant subunits in cerebellar cultures caused PC death. We hypothesized that the cell death was caused by excessive Ca^{2+} influx through the following steps. As cultured PCs spontaneously generate action potentials, which increase basal $[Ca^{2+}]_i$ (Schilling *et al.* 1991; Supplemental Fig. S4*B* and *C* and Table 1), the broadening of action potentials by R424H mutant expression would cause increased Ca^{2+} influx via excessive activation of voltage-gated Ca^{2+} channels. This influx would lead to a defect of Ca^{2+} homeostasis in PCs, resulting in the cell death as a part of a stress response (Orrenius *et al.* 2003). Indeed, excessive Ca^{2+} influx triggered by the blockade of K^+ channels has been shown to induce cell death in several types of cells (Kim *et al.* 2000; Lajdova *et al.* 2004; Wang *et al.* 2011). To test this hypothesis, we performed calcium imaging (Fig. 8) and then rescue experiments of PC death using ω-agatoxin IVA, a specific blocker for the P/Q-type voltage-gated Ca^{2+} channels that mediate predominant Ca^{2+} currents in PCs (Mintz & Bean, 1993; Gillard *et al.* 1997; Fig. 9).

Calcium imaging was performed using cerebellar cultures loaded with fura-2 AM (see Methods). After a baseline recording (measurement of basal $[Ca^{2+}]_i$) for 8 min, cerebellar cultures were depolarized for 5 min by perfusion of high-K^+ ACSF (Fig. 8*B*). In basal conditions, $[Ca^{2+}]_i$ in R424H mutant-expressing PCs was approximately four times higher than in the control group (Fig. 8*Ca*; $P < 0.001$ in R424H *versus* GFP and in R424H *versus* WT). There were no significant differences in high-K^+-induced $[Ca^{2+}]_i$ elevation (~200 nM) between PCs expressing the R424H mutant and those expressing GFP alone or expressing WT subunits (Fig. 8*Cb*). The basal $[Ca^{2+}]_i$ of granule cells infected with the

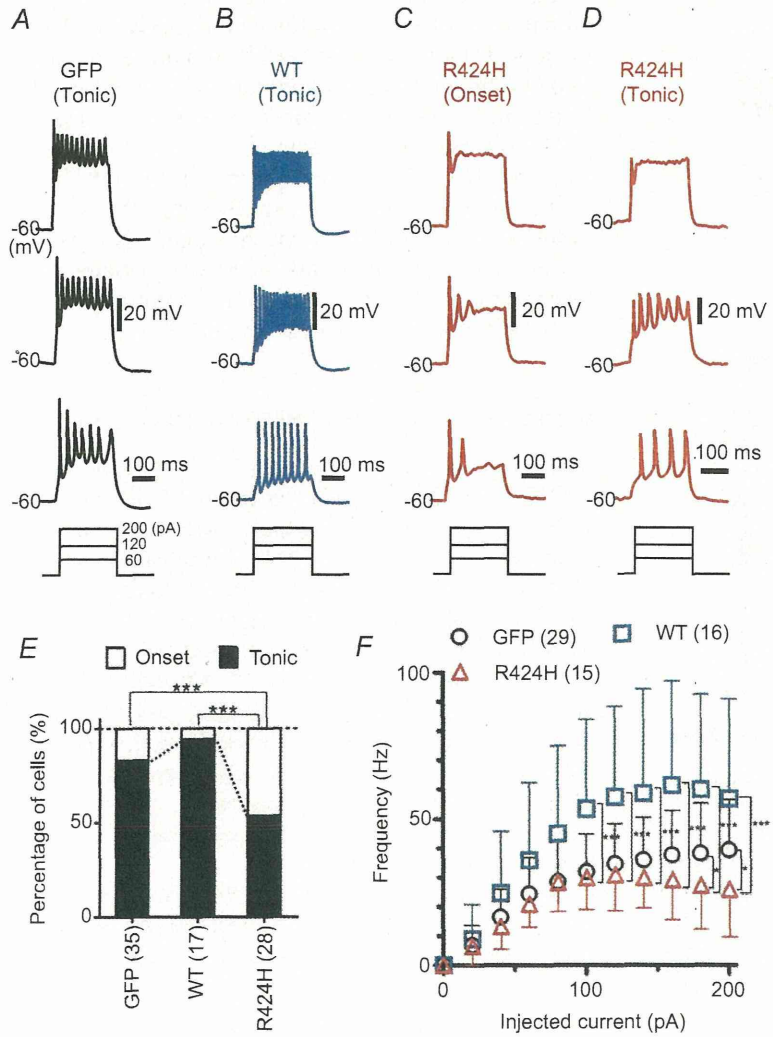

Figure 7. R424H mutant-expressing PCs exhibit altered firing patterns
A–D, representative firing patterns of PCs expressing GFP alone (*A*), WT subunits (*B*) or R424H mutant subunits (*C* and *D*). Approximately half of the R424H mutant-expressing PCs fired at the onset of current injection (onset-type; *C*). The action potentials were evoked by long depolarizing current injection (200 ms duration). The resting membrane potentials were adjusted to −60 mV. *E*, comparison of firing patterns. The χ^2 test was used for the statistical analyses. *F*, the firing frequency of the tonic-type cells is plotted as a function of injected current. $^*P < 0.05$ and $^{***}P < 0.001$.

lentiviruses was also measured, and there were no significant differences between R424H mutant-expressing and control cultures (GFP, 71.2 ± 41.2 nM, $n = 86$; WT, 69.7 ± 38.0 nM, $n = 118$; R424H, 63.6 ± 32.9 nM, $n = 72$; $P = 0.365$ between GFP and R424H; $P = 0.423$ between WT and R424H).

To examine whether the elevated basal $[Ca^{2+}]_i$ induced PC death in R424H mutant-expressing cultures, we performed a similar experiment to that in Fig. 2. In this experiment, ω-agatoxin IVA (0.2 μM) was added to the culture medium at DIV 2 (see Methods), and WT-expressing cultures were omitted to simplify the experimental design. Treatment of GFP-expressing cultures with ω-agatoxin IVA did not affect relative PC density (Fig. 9*D*, filled circles) but increased the branch number and the total length of dendrites at DIV 14 (Fig. 9*E* and *F*; filled circles in Fig. 9*I* and *J*), in good agreement with a previous report (Schilling *et al.* 1991; see Discussion). Treatment of R424H mutant-expressing cultures with ω-agatoxin IVA significantly increased relative PC density at DIV 11 and 14 (Fig. 9*D*, red triangles) and significantly rescued dendritic development in PCs (Fig. 9*G* and *H*; red triangles in Fig. 9*I* and *J*). These results clearly indicate that P/Q-type Ca^{2+} channels play a critical role in the PC death and impairment of dendrite development caused by R424H mutant expression, and support our hypothesis.

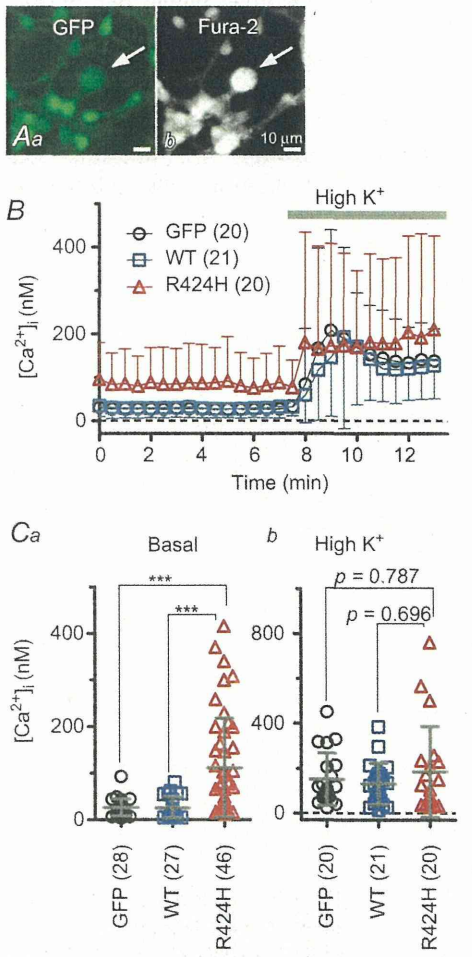

Figure 8. Significantly higher basal $[Ca^{2+}]_i$ in PCs expressing R424H mutant
A, representative fluorescence images of a fura-2 AM-loaded cerebellar culture expressing GFP alone. Arrows indicate PCs. *Aa*, GFP fluorescence (excitation, 470–495 nm; emission, 510–550 nm). *Ab*, fura-2 fluorescence (excitation, 375–385 nm; emission, 470–550 nm). *B*, the time course of free $[Ca^{2+}]_i$ in PCs. To depolarize PCs, high-K^+ ACSF (High K^+) was bath applied during the time indicated by the grey bar. *C*, summary of averaged $[Ca^{2+}]_i$ in PCs. Basal $[Ca^{2+}]_i$ was obtained as the average of a 7 min period from the beginning of the recordings (*Ca*), and elevated $[Ca^{2+}]_i$ from a 5 min period during high-K^+ ACSF perfusion (*Cb*). ***$P < 0.001$.

Discussion

In this study, we found that the expression of R424H mutant subunits in cerebellar cultures significantly impaired dendritic development and survival in PCs (Figs 2 and 3). Prior to cell death, R424H mutant-expressing PCs showed broadened action potential waveforms, altered firing properties and elevated basal $[Ca^{2+}]_i$ (Figs 6–8). Moreover, chronic inhibition of P/Q-type Ca^{2+} channels by ω-agatoxin IVA rescued the PC death and dendritic maldevelopment caused by expression of R424H mutant subunits (Fig. 9). This is the first report to show that a missense mutation found in SCA13 patients induces maldevelopment of PC dendrites and eventually PC death, most probably due to elevated basal $[Ca^{2+}]_i$ in PCs.

Biophysical properties of R424H mutant channels

The biophysical properties of hKv3.3 channels with the R423H mutation, which corresponds to the R424H mutation in mKv3.3 channels, have been previously reported (Figueroa *et al.* 2010; Minassian *et al.* 2012). Our results in Supplemental Fig. S2 agreed well with the previous reports and suggest that the properties of R424H mutant mKv3.3 were essentially identical to those of R423H-mutant hKv3.3. Moreover, we found that coexpression of R424H mutant and WT subunits accelerated the inactivation kinetics and slowed recovery from inactivation compared with expression of WT subunits alone (Fig. 1). Therefore, we predict that the properties we found in R424H mutant mKv3.3 are shared with R423H mutant hKv3.3.

We confirmed that homomeric R424H mutant channels showed negligible currents and that R424H mutant subunits exerted a dominant-negative influence on WT mKv3.3 channels in *Xenopus* oocytes (Supplemental Fig. S2*A* and *B*; Figueroa *et al.* 2010, 2011). Very recently,

Zhao *et al.* (2013) reported that in heterologous expression systems using Chinese hamster ovary cells, the surface protein level of R423H mutant hKv3.3 channels is 30% of that of WT hKv3.3 and that the conductance density of the mutant is 16% of that of the WT. Therefore, we cannot exclude the possibility that the reduced surface expression of mKv3.3 channels by the mutation would also contribute to the broadening of action potentials (Fig. 6) and lower firing frequency (Fig. 7) in transduced PCs. However, the reduction of the conductance density cannot be explained fully by the reduced surface protein expression.

To explain the negligible activity and dominant-negative property of R424H mutant channels, we propose two hypothetical mechanisms. First, the positively charged arginine at position 424 in mKv3.3 may be a critical residue in the S4 segment, serving as a part of the voltage sensor domain (Seoh *et al.* 1996). The partial disruption of the sensor domain by R424H mutation would make the subunits less sensitive to membrane voltage changes, resulting in the loss of channel function. Second, an arginine residue at position 174 in the S4 segment of KAT1, which is a voltage-gated K^+ channel in *Arabidopsis*, plays an essential role in the appropriate integration of the S3 and S4 segment into the endoplasmic reticulum membrane (Sato *et al.* 2003). Given that the R174 is homologous to R424 in mKv3.3, defective membrane insertion of R424H mutant subunits could occur in *Xenopus* oocytes, leading to a defect in channel activity.

Purkinje cell death by R424H mutant expression and the inhibition by blockade of P/Q-type voltage-gated Ca^{2+} channels

In this study, we revealed that expression of R424H mutant subunits caused cell death and impaired dendritic growth in PCs (Figs 2 and 3) and that these effects were reversed by the blockade of P/Q-type Ca^{2+} channels (Fig. 9). Addition of ω-agatoxin IVA also enhanced dendritic elongation in PCs expressing GFP alone (Fig. 9*E* and *F*; filled circles in Fig. 9*I* and *J*). Together with a previous report showing that chronic application of TTX in cerebellar cultures caused dendritic elongation in PCs (Schilling *et al.* 1991), activation of P/Q-type Ca^{2+} channels by neuronal activity may adversely influence dendritic elongation in PCs. Addition of ω-agatoxin IVA in R424H mutant-expressing cultures did not completely restore PC survival rates

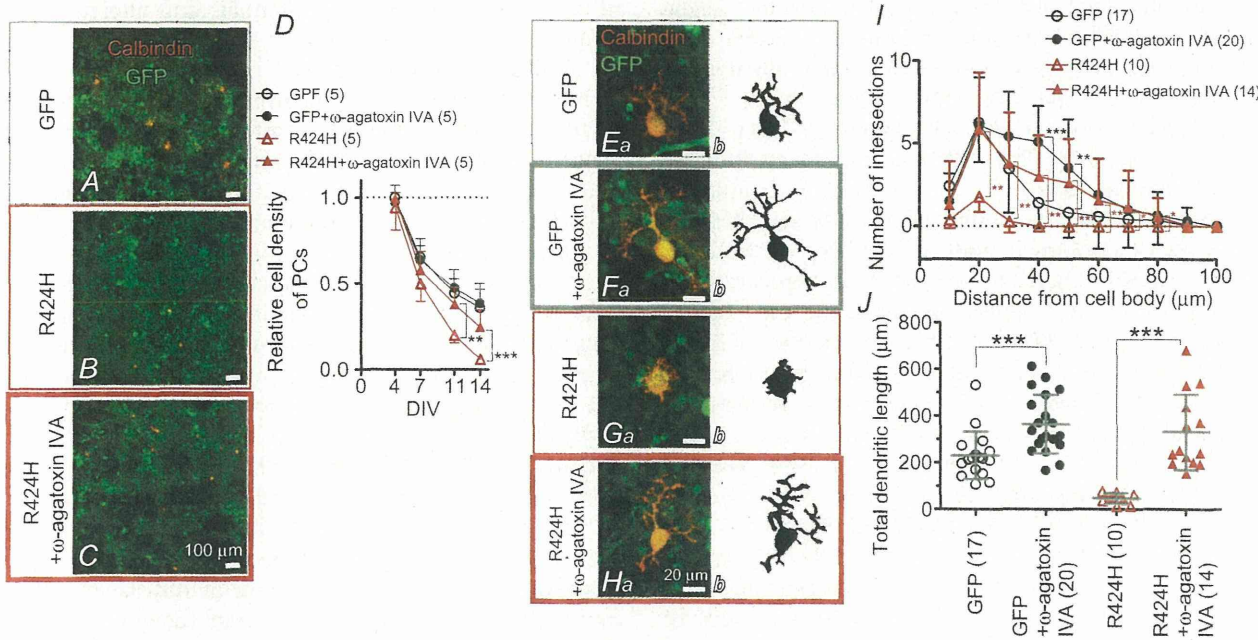

Figure 9. Pharmacological blockade of P/Q-type Ca^{2+} channels rescues the PC death and dendritic maldevelopment caused by expression of R424H mutant
A–C, cerebellar cultures expressing GFP alone (*A*) or R424H mutant with GFP (*B* and *C*). The cultures were immunostained for calbindin at DIV 14. In *C*, ω-agatoxin IVA was added to the culture medium every other day from DIV 2. *D*, relative cell density of PCs plotted as a function of DIV. The density was normalized to the value of PCs expressing GFP alone at DIV 4. *E–H*, calbindin-immunolabelled PCs expressing GFP alone (*Ea* and *Fa*) or R424H mutant subunits with GFP (*Ga* and *Ha*) at DIV 14. Morphologies of PCs are depicted in the right-hand panels for clarity. In *F* and *H*, ω-agatoxin IVA was added. *I*, and *J*, summary of dendrite complexity measured by Sholl analysis (*I*) and of total dendritic length (*J*). $^*P < 0.05$, $^{**}P < 0.01$, and $^{***}P < 0.001$.

(Fig. 9*D*). This may be because some Ca^{2+} currents in cultured PCs are mediated by Ca^{2+} channels other than the P/Q-type (Gillard *et al.* 1997), and activation of these channels may contribute to PC death. We therefore performed the same rescue experiments using $CdCl_2$ (0.2 mM; a non-selective Ca^{2+} channel blocker) or a combination of ω-agatoxin IVA and verapamil hydrochloride (0.02 mM; an L-type Ca^{2+} channel blocker), but these chemicals markedly deteriorated the viability and development of cerebellar cultures within 3 DIV (data not shown).

In contrast to PCs, there were no significant decreases in the numbers of granule cells upon R424H mutant expression (Fig. 2*E*). This may be because granule cells do not express endogenous mKv3.3 channels with which R424H mutant subunits form oligomeric channels (Supplemental Fig. S3*C*), resulting in the absence of the dominant-negative influence on the endogenous channels by the expression of mutant channel subunits.

Comparison with preceding papers on Kv3.3 knockout mice and zebrafish expressing mutant Kv3.3

In contrast to the impaired dendritic development in R424H mutant-expressing PCs (Fig. 3*Cb″* and *D*), the cerebellum of Kv3.3 knockout mice shows neither dendritic shrinkage of PCs nor cerebellar atrophy (Zagha *et al.* 2010). Furthermore, the knockout mice display only moderate motor dysfunction and no ataxic phenotype, although SCA13 patients show severe ataxia (Joho *et al.* 2006; Hurlock *et al.* 2008; Waters & Pulst, 2008; Figueroa *et al.* 2010). This difference may be attributable to the following factors. In PCs, mKv3.3 is thought to form heteromultimeric channels by assembling with Kv3.1 and/or Kv3.4 (Goldman-Wohl *et al.* 1994; Weiser *et al.* 1994), and Kv3 channels contribute to repolarization of both somatic Na^+ spikes and dendritic Ca^{2+} spikes (McKay & Turner, 2004). Genetic elimination of Kv3.3 subunits may be insufficient to exhibit the dendritic shrinkage and severe ataxia phenotypes because of functional compensation by Kv3.1 and Kv3.4 in PCs (Goldman-Wohl *et al.* 1994; Weiser *et al.* 1994; Martina *et al.* 2003). We detected the expression of Kv3.4 subunits in cultured PCs (Supplemental Fig. S3*D*). It is therefore reasonable to hypothesize that R424H mutant subunits form heteromultimeric channels not only with endogenous mKv3.3 but also with other members of Kv3.3, including Kv3.4, resulting in total inhibition of the K^+ channel activity in PCs. This may account for the differences in the morphological phenotypes of PCs in our results *versus* the knockout mice.

Zebrafish expressing infant-onset mutant zebrafish Kv3.3 (homologous to the F448L mutant in SCA13 patients) in spinal motoneurons show defective axonal pathfinding (Issa *et al.*, 2012). Indeed, the zebrafish is an interesting model for understanding the effects of mutant Kv3.3 expression in spinal motoneurons. However, as they used a motoneuron-specific enhancer of *Mnx1* (*Hb9*) gene, the exogenous proteins were not expressed in the cerebellar neurons. To examine the effects of mutant Kv3.3 in the cerebellum, it would be necessary to express the mutant protein directly in the cerebellar neurons using a different method.

Comparison of our culture results with SCA13 patients harbouring the R423H mutation

Spinocerebellar ataxia type 13 patients harbouring the R423H mutation generally show early-onset, slow-progressive ataxia and cerebellar atrophy (Figueroa *et al.* 2010, 2011). Our immunohistochemical analyses demonstrated that expression of R424H mutant subunits impaired dendritic development and induced cell death in cultured PCs (Figs 2 and 3). Those defects may be responsible for the cerebellar atrophy and ataxia observed in SCA13 patients, although it is necessary to verify that similar impairments are also observed in post-mortem cerebellum of the patients.

In functional aspects, we found that expression of R424H mutant subunits significantly decreased outward current mediated by voltage-gated K^+ channels, reduced sEPSCs, broadened action potentials and altered firing properties (Figs 4–7 and Table 2), suggesting the existence of similar functional changes in SCA13 patients. As PCs are the sole output neurons from the cerebellar cortex and make inhibitory synaptic contacts directly onto neurons in the deep cerebellar nuclei and the vestibular nuclei in the brainstem, PCs play crucial roles in motor co-ordination (Zheng & Raman, 2010). Accordingly, it is easily assumed that the reduction of spontaneous excitatory inputs and the changed firing properties in PCs disrupt synaptic transmission to neurons in the deep cerebellar nuclei and vestibular nuclei, resulting in impaired motor co-ordination. To examine the effects of the R424H mutation on electrophysiological properties of PCs and animal behaviour, we tried expressing R424H mutant subunits in PCs *in vivo* by directly injecting the virus solution into mouse cerebellar cortex as described in our previous papers (Torashima *et al.* 2006, 2008; Shuvaev *et al.* 2011). However, despite the presence of the infection, sufficient overexpression of mKv3.3 channels and apparent ataxia were not observed (data not shown). This may be because endogenous mKv3.3 proteins are abundantly expressed in PCs and the overexpression failed to reach the endogenous protein level. Efficient reduction of K^+ currents in PCs *in vivo* as observed in cultured PCs may be attained by using a different type of viral vector, such as adeno-associated virus vectors (Nathanson *et al.* 2009). Alternatively, K^+ currents in PCs *in vivo* may be effectively decreased using viral vector-mediated

expressions of R424H mutant subunits in *Kv3.3*$^{-/-}$ or *Kv3.3*$^{+/-}$ mice, which express no mKv3.3 proteins or only half the normal amount.

Currently, three different missense mutations in hKv3.3 channels have been reported from distinct pedigrees, and the disease onset and clinical phenotypes also differ among them (Waters *et al.* 2006; Figueroa *et al.* 2010, 2011). In the present study, we focused on only one mutation (R423H in hKv3.3) because of the drastic changes it induced in channel properties in the *Xenopus* oocyte expression system and its early-onset phenotype in SCA13 patients. Further studies of the effects of other mutants (R420H and F448L in hKv3.3) on cultured PCs may provide explanations for the differences in the disease phenotypes.

Possible significance of this study

We developed an *in vitro* SCA13 model using mouse cerebellar cultures and lentivirus vector-mediated gene expression. This model has advantages over *in vivo* models, such as transgenic mice, in the ease of controlling culture conditions by applying chemical compounds. Therefore, this model would be useful in screening drugs for SCA13 and in detailed investigations of the signalling cascades that promote the observed cell death. Given that blockade of P/Q-type Ca^{2+} channels rescued the phenotypes found in this research, the channel blockers may be potential therapeutic drugs for SCA13. Furthermore, this culture method, in combination with virus-mediated gene expression, may be applicable to the study of other types of hereditary spinocerebellar ataxia.

References

Armstrong CM & Bezanilla F (1974). Charge movement associated with the opening and closing of the activation gates of the Na channels. *J Gen Physiol* **63**, 533–552.

Ashcroft FM (2006). From molecule to malady. *Nature* **440**, 440–447.

Chang SY, Zagha E, Kwon ES, Ozaita A, Bobik M, Martone ME, Ellisman MH, Heintz N & Rudy B (2007). Distribution of Kv3.3 potassium channel subunits in distinct neuronal populations of mouse brain. *J Comp Neurol* **502**, 953–972.

Costa PF, Emilio MG, Fernandes PL, Ferreira HG & Ferreira KG (1989). Determination of ionic permeability coefficients of the plasma membrane of *Xenopus laevis* oocytes under voltage clamp. *J Physiol* **413**, 199–211.

Desai R, Kronengold J, Mei J, Forman SA & Kaczmarek LK (2008). Protein kinase C modulates inactivation of Kv3.3 channels. *J Biol Chem* **283**, 22283–22294.

Drummond GB (2009). Reporting ethical matters in *The Journal of Physiology*: standards and advice. *J Physiol* **587**, 713–719.

Erisir A, Lau D, Rudy B & Leonard CS (1999). Function of specific K^+ channels in sustained high-frequency firing of fast-spiking neocortical interneurons. *J Neurophysiol* **82**, 2476–2489.

Figueroa KP, Minassian NA, Stevanin G, Waters M, Garibyan V, Forlani S, Strzelczyk A, Bürk K, Brice A, Dürr A, Papazian DM & Pulst SM (2010). KCNC3: phenotype, mutations, channel biophysics—a study of 260 familial ataxia patients. *Hum Mutat* **31**, 191–196.

Figueroa KP, Waters MF, Garibyan V, Bird TD, Gomez CM, Ranum LP, Minassian NA, Papazian DM & Pulst SM (2011). Frequency of KCNC3 DNA variants as causes of spinocerebellar ataxia 13 (SCA13). *PLoS One* **6**, e17811.

Fry M, Boegle AK & Maue RA (2007). Differentiated pattern of sodium channel expression in dissociated Purkinje neurons maintained in long-term culture. *J Neurochem* **101**, 737–748.

Gillard SE, Volsen SG, Smith W, Beattie RE, Bleakman D & Lodge D (1997). Identification of pore-forming subunit of P-type calcium channels: an antisense study on rat cerebellar Purkinje cells in culture. *Neuropharmacology* **36**, 405–409.

Gimenez-Cassina A, Lim F & Diaz-Nido J (2007). Gene transfer into Purkinje cells using herpesviral amplicon vectors in cerebellar cultures. *Neurochem Int* **50**, 181–188.

Goldman-Wohl DS, Chan E, Baird D & Heintz N (1994). Kv3.3b: a novel Shaw type potassium channel expressed in terminally differentiated cerebellar Purkinje cells and deep cerebellar nuclei. *J Neurosci* **14**, 511–522.

Grynkiewicz G, Poenie M & Tsien RY (1985). A new generation of Ca^{2+} indicators with greatly improved fluorescence properties. *J Biol Chem* **260**, 3440–3450.

Hanawa H, Hematti P, Keyvanfar K, Metzger ME, Krouse A, Donahue RE, Kepes S, Gray J, Dunbar CE, Persons DA & Nienhuis AW (2004). Efficient gene transfer into rhesus repopulating hematopoietic stem cells using a simian immunodeficiency virus-based lentiviral vector system. *Blood* **103**, 4062–4069.

Harada KH, Ishii TM, Takatsuka K, Koizumi A & Ohmori H (2006). Effects of perfluorooctane sulfonate on action potentials and currents in cultured rat cerebellar Purkinje cells. *Biochem Biophys Res Commun* **351**, 240–245.

Hawley RG, Lieu FH, Fong AZ & Hawley TS (1994). Versatile retroviral vectors for potential use in gene therapy. *Gene Ther* **1**, 136–138.

Hille B (2001). *Ion Channels of Excitable Membranes*. Sinauer, Sunderland, MA.

Hirai H & Launey T (2000). The regulatory connection between the activity of granule cell NMDA receptors and dendritic differentiation of cerebellar Purkinje cells. *J Neurosci* **20**, 5217–5224.

Hirano T & Kasono K (1993). Spatial distribution of excitatory and inhibitory synapses on a Purkinje cell in a rat cerebellar culture. *J Neurophysiol* **70**, 1316–1325.

Hirano T, Kubo Y & Wu MM (1986). Cerebellar granule cells in culture: monosynaptic connections with Purkinje cells and ionic currents. *Proc Natl Acad Sci U S A* **83**, 4957–4961.

Hodgkin AL & Katz B (1949). The effect of sodium ions on the electrical activity of giant axon of the squid. *J Physiol* **108**, 37–77.

Hurlock EC, McMahon A & Joho RH (2008). Purkinje-cell-restricted restoration of Kv3.3 function restores complex spikes and rescues motor coordination in *Kcnc3* mutants. *J Neurosci* **28**, 4640–4648.

Issa FA, Mock AF, Sagasti A & Papazian DM (2012). Spinocerebellar ataxia type 13 mutation that is associated with disease onset in infancy disrupts axonal pathfinding during neuronal development. *Dis Model Mech* **5**, 921–929.

Joho RH, Street C, Matsushita S & Knöpfel T (2006). Behavioral motor dysfunction in Kv3-type potassium channel-deficient mice. *Genes Brain Behav* **5**, 472–482.

Kim JA, Kang YS, Jung MW, Kang GH, Lee SH & Lee YS (2000). Ca^{2+} influx mediates apoptosis induced by 4-aminopyridine, a K^+ channel blocker, in HepG2 human hepatoblastoma cells. *Pharmacology* **60**, 74–81.

Kubo Y & Murata Y (2001). Control of rectification and permeation by two distinct sites after the second transmembrane region in Kir2.1 K^+ channel. *J Physiol* **531**, 645–660.

Lajdova I, Chorvat D Jr, Spustova V & Chorvatova A (2004). 4-Aminopyridine activates calcium influx through modulation of the pore-forming purinergic receptor in human peripheral blood mononuclear cells. *Can J Physiol Pharmacol* **82**, 50–56.

McKay BE & Turner RW (2004). Kv3 K^+ channels enable burst output in rat cerebellar Purkinje cells. *Eur J Neurosci* **20**, 729–739.

MacKinnon R (1991). Determination of the subunit stoichiometry of a voltage-activated potassium channel. *Nature* **350**, 232–235.

Martina M, Yao GL & Bean BP (2003). Properties and functional role of voltage-dependent potassium channels in dendrites of rat cerebellar Purkinje neurons. *J Neurosci* **23**, 5698–5707.

Mellor JR, Merlo D, Jones A, Wisden W & Randall AD (1998). Mouse cerebellar granule cell differentiation: electrical activity regulates the $GABA_A$ receptor $\alpha 6$ subunit gene. *J Neurosci* **18**, 2822–2833.

Mikuni T, Uesaka N, Okuno H, Hirai H, Deisseroth K, Bito H & Kano M (2013). Arc/Arg3.1 is a postsynaptic mediator of activity-dependent synapse elimination in the developing cerebellum. *Neuron* **78**, 1024–1035.

Minassian NA, Lin MC & Papazian DM (2012). Altered Kv3.3 channel gating in early-onset spinocerebellar ataxia type 13. *J Physiol* **590**, 1599–1614.

Mintz IM & Bean BP (1993). Block of calcium channels in rat neurons by synthetic omega-Aga-IVA. *Neuropharmacology* **32**, 1161–1169.

Mullen RJ, Buck CR & Smith AM (1992). NeuN, a neuronal specific nuclear protein in vertebrates. *Development* **116**, 201–211.

Nathanson JL, Yanagawa Y, Obata K & Callaway EM (2009). Preferential labelling of inhibitory and excitatory cortical neurons by endogenous tropism of adeno-associated virus and lentivirus vectors. *Neuroscience* **161**, 441–450.

Orrenius S, Zhivotovsky B & Nicotera P (2003). Regulation of cell death: the calcium–apoptosis link. *Nat Rev Mol Cell Biol* **4**, 552–565.

Rae JL & Shepard AR (2000). Kv3.3 potassium channels in lens epithelium and corneal endothelium. *Exp Eye Res* **70**, 339–348.

Rudy B & McBain CJ (2001). Kv3 channels: voltage-gated K^+ channels designed for high-frequency repetitive firing. *Trends Neurosci* **24**, 517–526.

Sato M, Suzuki K, Yamazaki H & Nakanishi S (2005). A pivotal role of calcineurin signalling in development and maturation of postnatal cerebellar granule cells. *Proc Natl Acad Sci U S A* **102**, 5874–5879.

Sato Y, Sakaguchi M, Goshima S, Nakamura T & Uozumi N (2003). Molecular dissection of the contribution of negatively and positively charged residues in S2, S3, and S4 to the final membrane topology of the voltage sensor in the K^+ channel, KAT1. *J Biol Chem* **278**, 13227–13234.

Sawada Y, Kajiwara G, Iizuka A, Takayama K, Shuvaev AN, Koyama C & Hirai H (2010). High transgene expression by lentiviral vectors causes maldevelopment of Purkinje cells in vivo. *Cerebellum* **9**, 291–302.

Schilling K, Dickinson MH, Connor JA & Morgan JI (1991). Electrical activity in cerebellar cultures determines Purkinje cell dendritic growth patterns. *Neuron* **7**, 891–902.

Seoh SA, Sigg D, Papazian DM & Bezanilla F (1996). Voltage-sensing residues in the S2 and S4 segments of the *Shaker* K^+ channel. *Neuron* **16**, 1159–1167.

Sholl DA (1953). Dendritic organization in the neurons of the visual and motor cortices of the cat. *J Anat* **87**, 387–406.

Shuvaev AN, Horiuchi H, Seki T, Goenawan H, Irie T, Iizuka A, Sakai N & Hirai H (2011). Mutant PKCγ in spinocerebellar ataxia type 14 disrupts synapse elimination and long-term depression in Purkinje cells *in vivo*. *J Neurosci* **31**, 14324–14334.

Szymczak AL, Workman CJ, Wang Y, Vignali KM, Dilioglou S, Vanin EF & Vignali DA (2004). Correction of multi-gene deficiency in vivo using a single 'self-cleaving' 2A peptide-based retroviral vector. *Nat Biotechnol* **22**, 589–594.

Tabata T, Sawada S, Araki K, Bono Y, Furuya S & Kano M (2000). A reliable method for culture of dissociated mouse cerebellar cells enriched for Purkinje neurons. *J Neurosci Methods* **104**, 45–53.

Takayama K, Torashima T, Horiuchi H & Hirai H (2008). Purkinje-cell-preferential transduction by lentiviral vectors with the murine stem cell virus promoter. *Neurosci Lett* **443**, 7–11.

Torashima T, Iizuka A, Horiuchi H, Mitsumura K, Yamasaki M, Koyama C, Takayama K, Iino M, Watanabe M & Hirai H (2009). Rescue of abnormal phenotypes in $\delta 2$ glutamate receptor-deficient mice by the extracellular N-terminal and intracellular C-terminal domains of the $\delta 2$ glutamate receptor. *Eur J Neurosci* **30**, 355–365.

Torashima T, Koyama C, Iizuka A, Mitsumura K, Takayama K, Yanagi S, Oue M, Yamaguchi H & Hirai H (2008). Lentivector-mediated rescue from cerebellar ataxia in a mouse model of spinocerebellar ataxia. *EMBO Rep* **9**, 393–399.

Torashima T, Okoyama S, Nishizaki T & Hirai H (2006). In vivo transduction of murine cerebellar Purkinje cells by HIV-derived lentiviral vectors. *Brain Res* **1082**, 11–22.

Wang W, Xiao J, Adachi M, Liu Z & Zhou J (2011). 4-Aminopyridine induces apoptosis of human acute myeloid leukemia cells via increasing $[Ca^{2+}]_i$ through P_2X_7 receptor pathway. *Cell Physiol Biochem* **28**, 199–208.

Waters MF, Minassian NA, Stevanin G, Figueroa KP, Bannister JP, Nolte D, Mock AF, Evidente VG, Fee DB, Müller U, Dürr A, Brice A, Papazian DM & Pulst SM (2006). Mutations in voltage-gated potassium channel KCNC3 cause degenerative and developmental central nervous system phenotypes. *Nat Genet* **38**, 447–451.

Waters MF & Pulst SM (2008). SCA13. *Cerebellum* **7**, 165–169.

Weiser M, Vega-Saenz de Miera E, Kentros C, Moreno H, Franzen L, Hillman D, Baker H & Rudy B (1994). Differential expression of Shaw-related K^+ channels in the rat central nervous system. *J Neurosci* **14**, 949–972.

Zagha E, Manita S, Ross WN & Rudy B (2010). Dendritic Kv3.3 potassium channels in cerebellar Purkinje cells regulate generation and spatial dynamics of dendritic Ca^{2+} spikes. *J Neurophysiol* **103**, 3516–3525.

Zhao J, Zhu J & Thornhill WB (2013). Spinocerebellar ataxia-13 Kv3.3 potassium channels: arginine-to-histidine mutations affect both functional and protein expression on the cell surface. *Biochem J* **454**, 259–265.

Zheng N & Raman IM (2010). Synaptic inhibition, excitation, and plasticity in neurons of the cerebellar nuclei. *Cerebellum* **9**, 56–66.

Additional Information

Competing interests

None declared.

Author contributions

T.I. and H.H. conceived and designed experiments. T.I. and Y.M. performed experiments. T.I. collected and analysed data. T.I., Y.S. and H.H. wrote the paper.

Funding

This work was supported by Health Labour Sciences Research Grant (T.I.), JSPS KAKENHI grant numbers 24790230 (T.I.) and 19670003 (H.H.), and JSPS Funding Program for Next Generation World-Leading Researchers (LS021 to H.H.).

Acknowledgements

The lentiviral vector and MSCV promoter were provided by St Jude Children's Research Hospital and the American National Red Cross, respectively. We thank Dr L. K. Kaczmarek for mouse Kv3.3 cDNA and Dr K. Nakajo for technical advice and valuable comments on electrophysiological recording from *Xenopus* oocytes.